Resolvin D2 Enhances Postischemic Revascularization While Resolving Inflammation

BACKGROUND: Resolvins are lipid mediators generated by leukocytes during the resolution phase of inflammation. They have been shown to regulate the transition from inflammation to tissue repair; however, it is unknown whether resolvins play a role in tissue revascularization following ischemia.

METHODS: We used a murine model of hind limb ischemia (HLI), coupled with laser Doppler perfusion imaging, microcomputed tomography, and targeted mass spectrometry, to assess the role of resolvins in revascularization and inflammation resolution.

RESULTS: In mice undergoing HLI, we identified resolvin D2 (RvD2) in bone marrow and skeletal muscle by mass spectrometry (n=4–7 per group). We also identified RvD2 in skeletal muscle biopsies from humans with peripheral artery disease. Monocytes were recruited to skeletal muscle during HLI and isolated monocytes produced RvD2 in a lipoxygenase-dependent manner. Exogenous RvD2 enhanced perfusion recovery in HLI and microcomputed tomography of limb vasculature revealed greater volume, with evidence of tortuous arterioles indicative of arteriogenesis (n=6–8 per group). Unlike other treatment strategies for therapeutic revascularization that exacerbate inflammation, RvD2 did not increase vascular permeability, but reduced neutrophil accumulation and the plasma levels of tumor necrosis factor-α and granulocyte macrophage colony-stimulating factor. In mice treated with RvD2, histopathologic analysis of skeletal muscle of ischemic limbs showed more regenerating myocytes with centrally located nuclei. RvD2 enhanced endothelial cell migration in a Rac-dependent manner, via its receptor, GPR18, and *Gpr18*-deficient mice had an endogenous defect in perfusion recovery following HLI. Importantly, RvD2 rescued defective revascularization in diabetic mice.

CONCLUSIONS: RvD2 stimulates arteriogenic revascularization during HLI, suggesting that resolvins may be a novel class of mediators that both resolve inflammation and promote arteriogenesis.

Michael J. Zhang, PhD*
Brian E. Sansbury, PhD*
Jason Hellmann, PhD
James F. Baker
Luping Guo, MD
Caitlin M. Parmer
Joshua C. Prenner
Daniel J. Conklin, PhD
Aruni Bhatnagar, PhD
Mark A. Creager, MD
Matthew Spite, PhD

*Drs Zhang and Sansbury contributed equally to this study and share first-authorship.

Correspondence to: Matthew Spite, PhD, Harvard Institutes of Medicine, 77 Ave Louis Pasteur, HIM830 Boston, MA 02115. E-mail mspite@bwh.harvard.edu

Sources of Funding, see page 678

Key Words: imaging techniques
- inflammation
- revascularization
- peripheral vascular diseases

Clinical Perspective

What Is New?

- Resolvins are a family of lipid mediators biosynthesized from omega-3 polyunsaturated fatty acids that promote the resolution phase of inflammation. Here, we found that resolvin D2 (RvD2) promotes limb revascularization during ischemia while resolving inflammation and has direct receptor-dependent (ie, GPR18) actions on endothelial cells.
- We identified that RvD2 is produced in the skeletal muscle in a murine model of limb ischemia, and in patients with peripheral artery disease, as well. We found that RvD2 increases tissue perfusion by promoting arteriogenesis (ie, collateral artery growth) and that it rescues defective revascularization in diabetic mice.

What Are the Clinical Implications?

- Nonsurgical therapeutic strategies to increase limb perfusion in patients with peripheral artery disease are limited, particularly in those with diabetes mellitus.
- Most mediators that promote revascularization also exacerbate inflammation, potentially limiting their therapeutic use in these chronic inflammatory diseases.
- Thus, RvD2 is unique in that it both promotes revascularization and resolves inflammation, which could inform the development of novel strategies for the clinical management of limb ischemia.

Arterial occlusion during peripheral artery disease (PAD) impairs tissue perfusion and, in its most advanced stage, can lead to critical limb ischemia (CLI) and limb loss.[1–3] Arteriogenesis (ie, collateral vessel growth) is an endogenous process that partially compensates for defects in tissue perfusion.[4] Arteriogenesis is stimulated by increased shear stress associated with diversion of blood flow proximal to the occlusion into preexisting collateral arteriolar connections, and by growth factors and cytokines, as well.[5,6] Although arteriogenesis partially compensates for reduced blood flow after occlusion, the endogenous process could be enhanced therapeutically.[5,7]

Arteriogenesis is tightly coupled to the inflammatory response; monocytes and macrophages recruited to the tissue secrete growth factors that promote endothelial cell migration and proliferation, and mural cell recruitment and differentiation, as well.[6] Monocytes are sufficient to enhance revascularization in mouse models of HLI, and mice deficient in monocyte chemotaxis (eg, *Ccr2*) have impaired perfusion recovery.[6,8–10] Several therapeutic strategies have been tested to increase arteriogenesis, including growth factors and mononuclear cells. However, the efficacy of these approaches has met limited success in large clinical trials, which could be related to the chronic inflammatory environment typically encountered in patients with PAD.[7] Importantly, most factors that promote revascularization are also proinflammatory and can increase atherosclerosis, potentially limiting their therapeutic use in patients with PAD.[7,11,12]

Recent studies indicate that resolution of inflammation is important for the transition to tissue repair during wound healing.[13] Resolution is an active process that involves the generation of proresolving lipid mediators, such as the resolvins.[14] Resolvins have receptor-dependent anti-inflammatory actions that include decreasing neutrophil trafficking to inflammatory loci and attenuating proinflammatory cytokine production.[14,15] They also stimulate macrophage-mediated clearance of apoptotic cells and promote tissue repair and regeneration.[13] Resolvins regulate leukocyte-endothelial interactions and have direct receptor-mediated signaling roles in endothelial cells.[16–18] Hence, we asked whether resolvins play a role in revascularization.

METHODS

Animals and Reagents

Male C57BL/6J (wild-type [WT]) mice, leptin receptor-deficient (*db/db*) mice, and 12/15-lipoxygenase (LOX)-deficient mice (*Alox15*^{tm1fun}) on a C57BL/6J background were purchased from Jackson Laboratories at 8 to 10 weeks of age. *Gpr18*-deficient mice and their WT littermates are on a mixed 129/SvEv-C57B/6 background. Resolvin D2 (RvD2; 7*S*,16*R*,17*S*-trihydroxy-4*Z*,8*E*,10*Z*,12*E*,14*E*,19*Z*-docosahexaenoic acid) was purchased from Cayman Chemical. All animal procedures were approved by the Harvard Medical Area Standing Committee on animals or the University of Louisville IACUC.

Surgical Hind Limb Ischemia Model

For the surgical induction of hind limb ischemia (HLI),[19] mice were anesthetized with 2% isoflurane (with 2 L/min O_2) and maintained on a temperature-controlled water blanket at 37°C. Depilatory cream was applied to the limbs and the area was sterilized by 70% ethanol applications. A 5-mm vertical skin incision was made lateral to the abdomen and superficial to the inguinal ligament. The inguinal fat pad was separated from the peritoneal lining to reveal the proximal femoral artery branching from the internal iliac artery. The femoral artery and vein were then separated from the membrane sheath, and 2 ligatures were tied around both vessels ≈2 mm apart.[20–22] Vessels were transected between the ligatures, and the skin incision was closed with 2 discontinuous sutures and bonded with *n*-butyl-ester cyanoacrylate. Sham-operated mice were opened, dissected, and closed without vessel ligature. In some cases, a less-severe model of HLI was used. For this, a 3-mm horizontal skin incision was made superficial to the medial right knee. The branch point where the femoral artery bifurcates into the saphenous artery and popliteal artery was exposed from its membrane sheath. The accompanying nerve was carefully avoided and a ligature was placed around the saphenous artery and vein immediately distal to the femoral bifurcation.

A second ligature was tied ≈1 mm below the first, and vessels were then transected between ligatures. The skin was then closed with sutures and cyanoacrylate. Buprenorphine (0.5 mg/kg) was given twice within 24 hours postsurgery. Twenty-four hours after surgery, mice were injected with either 0.9% saline vehicle (100 μL), or RvD2 in vehicle (1 ng/μL; 100 μL) subcutaneously and just superficial to the ligation site. Treatments were given daily until euthanasia.

Perfusion Imaging

Limb perfusion was assessed by laser Doppler perfusion imaging. For this, mice were anesthetized with isoflurane and placed on a dark scanning surface. Perfusion of the ventral surface of both right and left hind limbs was measured with a PeriScan PIM 2 laser Doppler device (Perimed). Images were acquired 1, 7, and 14 days after ligation. After acquisition, color-binned images of the mouse limbs were imported into ImageJ, and areas of blue, green, and red in the region of interest spanning the entire hind limb were enumerated. The value for the right ischemic limb was then normalized to the left (nonischemic) limb to calculate the percentage of recovery of blood perfusion for each mouse. For experiments with *Gpr18*-deficient mice and *db/db* mice, limb perfusion was measured by infrared laser speckle contrast analysis using a moorFLPI-2 full-field laser perfusion imager (Moor Instruments). Images were acquired immediately after ligation (day 0), 7 or 14 days after surgery. Images were analyzed by using the moorFLPI-2 Review Software, and the recovery of blood perfusion was calculated as described above.

Vascular Casting and Microcomputed Tomography Analysis

To visualize and quantitate the limb vasculature, we performed vascular casting, followed by microcomputed tomography (micro-CT) analysis.[23] For this, mice were given heparin (1000 U/mL; IP) as an anticoagulant and were subsequently sedated with sodium pentobarbital (50 mg/kg). The heart was then cannulated with a 15G needle and mice were perfused systemically with adenosine (100 μmol/L; 10 mL), followed by sodium nitroprusside (10 μmol/L) and then with bovine serum albumin (BSA; 0.05% wt/vol) at a flow rate of 5 mL/min.[19] Undiluted Microfil (FlowTech, Inc) was mixed with hardening solution, perfused, and allowed to solidify. The entire lower body was deskinned and fixed in formalin for 24 hours, which was followed by bone decalcification (Cal EX II) for 48 hours. Samples were then imaged with a MicroCAT II (Siemens) scanning at 80 kVp and 500 μA, with 2×2 binning for a pixel resolution of 1024×1024 with 34-μm voxel sizes. After thresholding of soft tissue, casted blood vessel voxel volumes were then quantified using Analyze (AnalyzeDirect). For whole-mount imaging of Microfil casted limbs, harvested limbs were placed in graded solutions of glycerol (40%, 60%, 80%, and 100%; changed every 24 hours) and images were acquired using a digital charge-coupled device camera (Nikon).

Histological Analysis of Ischemic Limbs

For histological analysis, mice undergoing HLI for 14 days were euthanized and their limbs were dissected. The hamstring muscles were excised and fixed in formalin and paraffin embedded. Three transverse cross sections of the muscles were mounted per slide, and 2 slides were analyzed per mouse. Gross examination of tissue injury was performed on hematoxylin and eosin–stained sections. The number of myocytes with centrally located nuclei indicates muscle regeneration, and this was used to assess the extent of limb damage and recovery with RvD2 treatment.[24] Five to 10 low-power fields were examined in each section, and the total number of myocytes with centrally located nuclei was determined and expressed as a percentage of the total myocytes per field.

Human Peripheral Artery Disease Cohort

PAD patients with stable intermittent claudication, and healthy control subjects, as well, were recruited as part of a prospective clinical trial investigating the effect of exercise training on skeletal muscle metabolism in PAD. The human study was approved by the institutional review board (#2010P001107) at Brigham and Women's Hospital, and all subjects gave signed informed consent. The diagnosis of PAD was made based on a resting ankle-brachial index of ≤0.90 or a decrease in ankle-brachial index of at least 20% following maximal exercise. Patients with diabetes mellitus and those with signs of critical limb ischemia were excluded. To minimize the risk of bleeding during the calf muscle biopsy, subjects were also excluded if they were taking warfarin. Healthy subjects were at least 50 years of age, had no known medical problems, and were ineligible if they had smoked within the past year. Subjects were recruited from clinical practices at Brigham and Women's Hospital and by advertisement.

Biopsy specimens were obtained from the medial head of the gastrocnemius. For PAD subjects, samples were taken from the more symptomatic leg or the leg with a lower ankle-brachial index if the subject experienced equal bilateral symptoms. Under local anesthesia, ≈100 to 150 mg of muscle tissue was collected using a 5-mm Bergstrom percutaneous muscle biopsy needle. Samples were immediately frozen in liquid nitrogen and stored at –80°C. Calf muscle biopsy samples were obtained from 15 subjects with PAD that completed the study and 7 healthy age-matched controls. The complete results of this ongoing clinical study will be reported separately.

Solid-Phase Extraction and LC-MS/MS Identification of Resolvins

To assess the formation of RvD2 and 17-hydroxydocosahexaenoic acid (17-HDHA), skeletal muscle biopsies from PAD patients or limb skeletal muscle tissues from mice undergoing HLI were collected and minced in ice-cold methanol. Bone marrow was isolated from femurs and tibias of mice undergoing HLI by flushing with ice-cold methanol. Before solid-phase extraction, internal deuterium-labeled standards (ie, d_5-RvD2 and d_8-5*S*-hydroxyeicosatetraenoic acid) were added to skeletal muscle, bone marrow, and monocyte samples (see below) to assess extraction recovery. Solid-phase extraction and liquid chromatography-tandem mass spectrometry (LC-MS/MS) analysis were performed essentially as described in Colas et al.[25] In brief, lipid mediators were extracted by using C18 solid-phase extraction cartridges and an automated extraction system (RapidTrace, Biotage). Methyl formate fractions were collected and the solvent was evaporated using a

stream of N_2 gas, followed by resuspension in methanol:water (50:50). Samples were then analyzed by LC-MS/MS using a Poroshell reverse-phase C18 column (100 mm×4.6 mm×2.7 μm; Agilent Technologies) equipped high-performance liquid chromatography system (Shimadzu) coupled to a QTrap 5500 mass spectrometer (AB Sciex). The mobile phase consisted of methanol:water:acetic acid (55:45:0.01 vol/vol/vol) and was ramped to 85:15:0.01 (vol/vol/vol) for 10 minutes, followed by ramping to 98:2:0.01 (vol/vol/vol) during the next 8 minutes and held for an additional 2 minutes. The entire sample elution was performed using a constant flow rate of 400 μL/min at a constant temperature of 50°C. The QTrap was operated in negative ionization mode using scheduled multiple reaction monitoring and transitions for RvD2 (375>215; 375>175) and 17-HDHA (343>245) coupled with information-dependent acquisition and enhanced product ion scanning. Mediators were identified using retention time and 6 diagnostic MS/MS ions, in comparison with identical authentic standards (Cayman Chemical). Concentration was determined by using standard curves generated for each mediator with synthetic standards after normalization of extraction recovery based on internal standards.

Splenic Monocyte Isolation and in Vitro Stimulation

To obtain a pure population of splenic monocytes, intact spleens were rapidly excised from anesthetized WT or *Alox15*-deficient mice and ruptured between 2 microscope slides. The spleen was then rubbed through a 40-μm cell strainer and rinsed with Pharmlyse to lyse red blood cells. After 5 minutes incubation in the dark at room temperature, the strained cells were washed with phosphate-buffered saline (PBS) containing 2 mmol/L EDTA and 0.5% BSA (MACS buffer). An EasySep mouse Monocyte Enrichment Kit (Stemcell Technologies) was then used to deplete nonmonocyte populations by antibody-biotin-magnetic bead separation. The remaining population was confirmed by flow cytometry to be ≈93% pure Ly-6C$^+$CCR2$^+$ monocytes. After isolation of splenic monocytes, cells were washed with Hanks Balanced Salt Solution to remove EDTA and to supplement calcium. Monocytes were then divided (1×10^5 cells per incubation) and stimulated with calcium ionophore (A23187; 10 μmol/L) and docosahexaenoic acid (DHA; 10 μmol/L) for 30 minutes at 37°C. The incubation was then terminated with 1.5 mL of ice-cold methanol and the samples were immediately frozen at –80°C for subsequent LC-MS/MS analysis (see above).

Flow Cytometry Analysis of Leukocytes in Ischemic Limbs

To identify leukocyte populations in muscle tissue, HLI was performed at as described above, and mice were euthanized after 3 days. The right hamstring muscles of the upper limb were then excised, weighed, and placed in enzyme digestion solution consisting of 500 U/mL collagenase II and 2.5 U/mL dispase II in 1800 μL of Hanks Balanced Salt Solution. Muscles were left to digest at 37°C for 1.5 hours. The digestate was then strained through a 40-μm cell strainer and washed with 2 mL of PBS with 1% BSA. The strained cells were incubated with Fc-block (anti-CD16/32) and then stained with fluorescein isothiocyanate anti-CCR2, APC anti-F4/80, APC/Cy7 anti-Ly-6G, and PerCP anti-CD45. After 30 minutes, cells were washed with 1 mL of PBS-BSA and analyzed by using a BD LSR II flow cytometer and FlowJo software.

Multiplex ELISA Analysis of Mouse Plasma

Mouse peripheral blood was collected by cardiac puncture, anticoagulated with EDTA, and centrifuged at 2000*g* for 20 minutes. The plasma supernatant was collected and frozen at –80°C. Multiplex ELISA analyses were then performed by Quansys Biosciences.

Matrigel Plug Angiogenesis Assay

To quantify angiogenesis, we used the Matrigel plug assay.[23] A 500-μL aliquot of Matrigel (Cultrex HC, Trevigen) was thawed on ice and mixed with either no additives, 50 U heparin + basic fibroblast growth factor (500 ng), or RvD2 (100 ng). The mixture was then loaded into syringes with an attached 25-gauge needle. Mice were anesthetized with isoflurane and hair was removed with depilatory cream on the right lateral abdomen. The Matrigel mixture was then injected subcutaneously and solidified into plugs for 20 minutes. After 7 days, mice were euthanized and the Matrigel plugs were excised. To release the infiltrated endothelial cells, Matrigel plugs were digested with 5 mg/mL of type I and II collagenase in 1 mL of Hanks Balanced Salt Solution for 1 hour at 37°C. Digested plugs were then strained with a 40-μm cell strainer and rinsed with PBS-BSA. The cell solution was incubated with Fc-block (anti-CD16/32) and then stained with PE anti-CD31 and PE/Cy7 anti-CD105. The cells were analyzed by flow cytometry as described above.

Endothelial Cell Migration and Proliferation Assays

To assess migration, mouse endothelial cells (MS1; ATCC) were seeded at 1×10^6 cells per well the night before experimentation in 3 mL of Dulbecco Modified Eagle Medium. With the use of a 200-μL pipette tip, 2 vertical scratches were made across the culture dish. The scratch was then imaged and the medium was replaced with fresh media containing vascular endothelial growth factor A (VEGF-A) (100 ng/mL) or RvD2 (0.1–10 nmol/L). In some experiments, the cells were preincubated with Rac inhibitor, NSC23766 (100 nmol/L), pertussis toxin (1 μg/mL), N$^\omega$-nitro-L-arginine methyl ester (100 μmol/L) or O-1918 (20 μmol/L) 30 minutes before stimulation with RvD2 (10 nmol/L). Eighteen hours later, the plates were imaged again. The 0-hour and 18-hour images were then processed by Photoshop (Adobe) with vertical lines demarcating migration of cells into the scratch site, and the width was determined using Image J (NIH). To assess proliferation, MS1 cells were seeded at 1×10^4 cells per well in 100 μL of Dulbecco Modified Eagle Medium containing 1% fetal bovine serum overnight. The next morning, cells were given fresh media containing VEGF-A (100 ng/mL) or RvD2 (0.1–10 nmol/L) and incubated at 37°C for 48 hour. Cell proliferation was measured using a Click-iT EdU kit (Life Technologies) and quantitated on a microplate reader (Biotek), whereas viability and total cell number were determined in separate assays using an MTT assay kit (Invitrogen). For quantitative reverse

transcription polymerase chain reaction analysis, cells were stimulated with or without VEGF-A (100 ng/mL) for 24 hours then lysed with Buffer RLT (Qiagen) containing 2-mercaptoethanol and processed as described below.

Assessment of Vascular Permeability

Vascular permeability was assessed in vivo using a modified Miles assay.[26,27] As with previous surgical procedures, mice were anesthetized with 2% isoflurane (2 L/min O_2) and maintained on a temperature-controlled water blanket at 37°C. The dorsal skin was shaved and the hair was removed with depilatory cream. Evan blue dye was administered by retro-orbital injection (100 μL, 1% in PBS) and after 5 minutes, 20 μL of PBS, histamine (25 ng/μL) or RvD2 (5 ng/μL) was injected subcutaneously into the dorsal skin. Mice were euthanized after 10 minutes by cervical dislocation and the dorsal skin was removed. The injection sites were collected by using a 12-mm biopsy punch and incubated in formamide at 55°C for 24 hours. Evan blue extravasation into the tissue was measured by absorption at 620 nm using a Nanodrop (Thermo) and is expressed as micrograms of Evan blue dye per cm^2 of skin.

Quantitative Reverse Transcription Polymerase Chain Reaction Analysis

Mouse hamstring muscles were harvested, snap-frozen in liquid N_2, and pulverized. The pulverized tissue was incubated and vortexed in TRIzol (Life Technologies) for 5 minutes. Tissue homogenates were then incubated with chloroform for 3 minutes and then centrifuged at 12 000*g* for 15 minutes at 4°C. The upper aqueous phase was transferred to a new tube and RNA was then purified with an RNeasy kit (Qiagen). Similarly, RNA from cell lysates collected in Buffer RLT (Qiagen) was purified with an RNeasy kit and RNA quality was checked by 260/280 UV absorbance ratio with a Nanodrop (Thermo). cDNA was prepared by PCR using avian myeloblastosis virus reverse transcriptase and oligoDT primers. Real-time amplification was performed with PerfeCTa SYBR Green FastMix (Quanta Biosciences) using a 7900HT Fast Real-time PCR system (Applied Biosystems). Commercially available primers were used for targeted analysis of *Emr1* or *Gpr18* (SA Biosciences). The hypoxanthine-guanine phosphoribosyltransferase (*Hprt*) housekeeping gene was used as internal quantitation control. Relative expression was calculated by using the $2^{-\Delta\Delta Ct}$ method.

Rac Activation Assay and Western Blotting

MS1 cells were cultured on 150-mm plates in 30 mL of Dulbecco Modified Eagle Medium with 10% fetal bovine serum until 50% confluence. Culture medium was then changed to 1% serum Dulbecco Modified Eagle Medium for 18 hours. Cells were either left unstimulated or stimulated with RvD2 (1 nmol/L) for 30 minutes. Plates were then rinsed with ice-cold PBS to halt the reaction. An activated GTP-bound Rac pull-down assay was performed using a Rac activation kit (Cell Biolabs). Subsequently, Rac pull-down samples were separated by sodium dodecyl sulfate-polyacrylamide gel electrophoresis and transferred to polyvinylidene difluoride membranes. The membrane was blocked overnight in Tris-buffered saline with 1% Tween 20 (TBS-T) and 5% powdered milk. Total Rac was then probed with anti-Rac antibodies (Cell Signaling Technologies) and anti-rabbit horseradish peroxidase in TBS-T with 1% BSA. Membranes were then developed with horseradish peroxidase substrate (Millipore) and scanned with a Typhoon bioimager (GE Healthcare). Densitometry analysis was performed using ImageJ.

The abundance of GPR18 protein in endothelial cells was measured by Western blot analysis. For this, confluent MS1 cells were lysed in radioimmunoprecipitation assay buffer with protease and phosphatase inhibitor cocktails (ThermoFisher Scientific) added. Samples were prepared at a concentration of 50 μg of protein in sample buffer with 100 mmol/L dithiothreitol, then separated by sodium dodecyl sulfate polyacrylamide gel electrophoresis and transferred to a polyvinylidene difluoride membrane. The membrane was blocked in TBS-T and 5% milk for 2 hours at room temperature and incubated overnight at 4°C in TBS-T and 5% milk with the primary anti-GPR18 (Abcam 174835) antibody. The secondary anti-rabbit horseradish peroxidase (Cell Signaling) antibody was incubated in TBS-T and 5% milk at room temperature for 1.5 hours. The blot was then developed using Luminata Forte (EMD Millipore) and x-ray film.

Statistics

Data are presented as mean±standard error of the mean. Parametric statistical analysis was performed in cases where cumulative data were normally distributed, as determined by D'Augostino and Pearson omnibus normality tests. Based on this, we assumed a normal distribution in individual assays of the same type but with smaller sample sizes. For this, multiple groups were compared using 1-way analysis of variance, followed by Tukey (comparing all groups) or Dunnett (comparing treatments versus control group) post hoc tests for contrasts of interest. For perfusion recovery, 2-way analysis of variance was performed, followed by Sidak multiple comparisons post hoc tests. For direct comparisons, an unpaired 2-tailed Student *t* test was used. In individual assays where normality could not be tested based on sample size without cumulative historical data, we used nonparametric Kruskal-Wallis tests, with Dunn multiple comparisons post hoc tests (comparing all groups) as indicated in the figure legends. In all cases, a $P<0.05$ was considered significant; exact *P* values for significant relationships are indicated in the figures. GraphPad Prism 6.0 was used for all statistical analysis.

RESULTS

RvD2 Is Generated in Ischemic Tissue in Both Mice and Humans

In acute sterile or infectious inflammation, D-series resolvins are generated by leukocytes during the resolution phase.[14] Their biosynthesis involves conversion of DHA to a 17-hydroperoxide (17-H(p)DHA) intermediate by 12/15-lipoxygenase (*Alox15*; 15-LOX type 1 in humans) (Figure 1A).[14–16] This intermediate is further converted to RvD2 by 5-LOX (Figure 1A). Because isch-

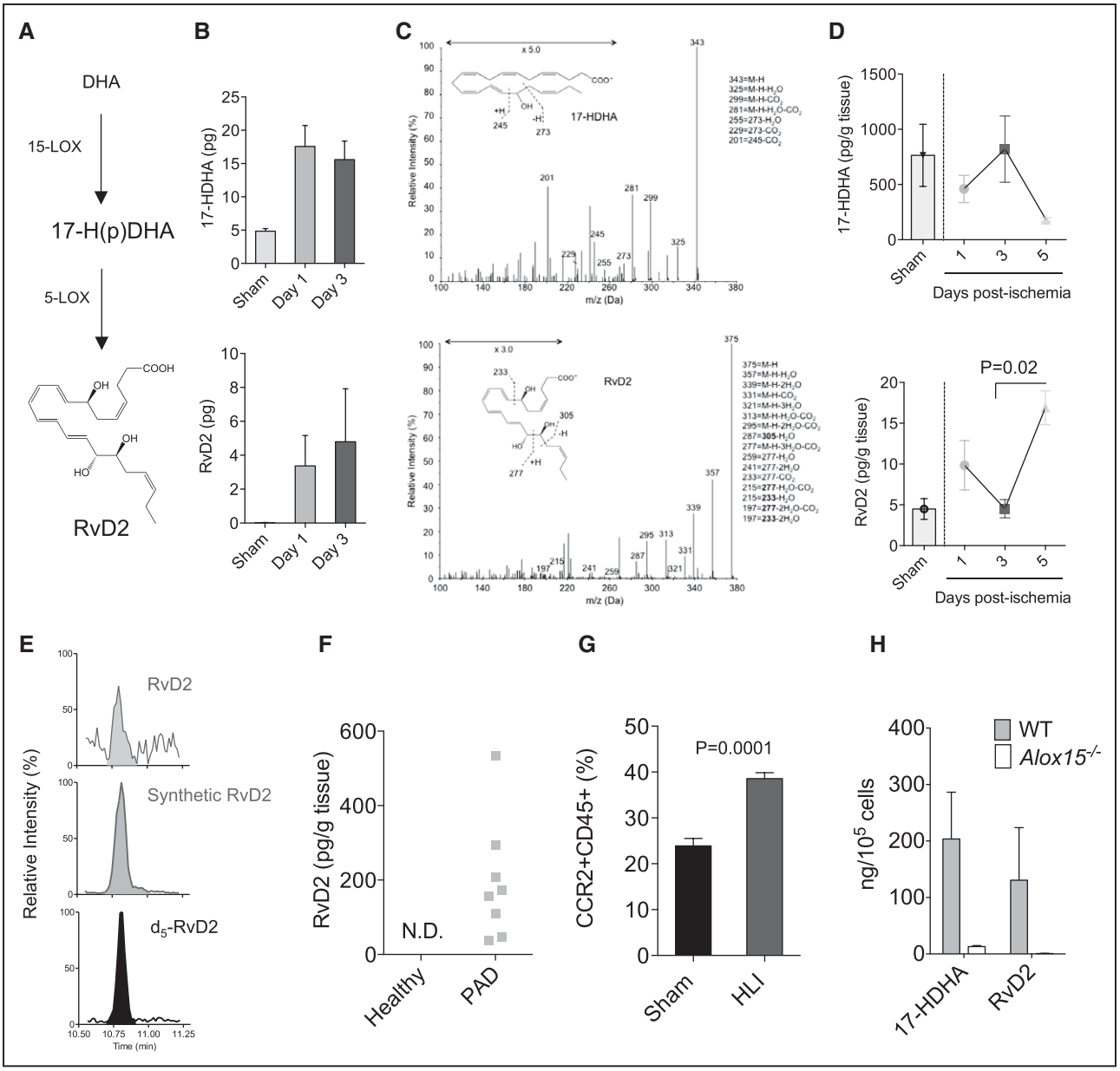

Figure 1. Biosynthesis of RvD2 in mice undergoing HLI and humans with peripheral artery disease.
A, Schematic of the RvD2 biosynthetic pathway, where docosahexaenoic acid (DHA) is converted to a 17-hydroperoxide (Hp) intermediate by 12/15-lipoxygenase (Alox15; 15-LOX type 1 in humans). This intermediate is converted to RvD2 by 5-LOX. **B,** Quantification of 17-HDHA and RvD2 in bone marrow of mice undergoing sham surgery or HLI. **C,** Representative MS/MS spectra of 17-HDHA and RvD2 generated in bone marrow during HLI (day 3), with structure and diagnostic ion assignments shown as inset. **D,** Time course of 17-HDHA and RvD2 formation in skeletal muscle of mice undergoing HLI. **E,** Representative multiple reaction monitoring (MRM) chromatogram used for identification of RvD2 in skeletal muscle biopsies of patients with peripheral artery disease (PAD), with external RvD2 standard and internal deuterium-labeled (d_5) RvD2 standard shown (retention time, 10.8 minutes). **F,** Quantification of RvD2 in PAD patients and healthy controls (N.D., not detected). **G,** Flow cytometry analysis of $CCR2^+CD45^+$ monocytes in skeletal muscle of mice undergoing HLI (day 3; % of total cell gate). **H,** Biosynthesis of 17-HDHA and RvD2 in splenic $CCR2^+$ monocytes isolated from WT or *Alox15*$^{-/-}$ mice. Data are mean±SEM; n=6 to 7/group/time point (**B** and **C**), n=3 (sham) and n=4 to 7/group/time point (**D**), 7 (healthy) or 15 (PAD)/group (**F**), and n=3 to 5/group (**G** and **H**). Statistical comparisons were made using nonparametric 1-way ANOVA (Kruskal-Wallis), followed by Dunn multiple comparisons post hoc tests (**D**) or by an unpaired 2-tailed Student *t* test (**G**). ANOVA indicates analysis of variance; 17-HDHA, 17-hydroxydocosahexaenoic acid; HLI, hind limb ischemia; MS/MS, tandem mass spectrometry; RvD2, resolvin D2; and SEM, standard error of the mean.

emia stimulates mobilization of immune cells from bone marrow that promote revascularization,[28] we first questioned whether RvD2 is generated in the bone marrow during ischemia. Indeed, we observed that RvD2 and its biosynthetic pathway marker, 17-HDHA, were generated in the ischemic limb bone marrow as early as 24

hours postsurgery (Figure 1B). Representative MS/MS spectra of 17-HDHA and RvD2 are shown in Figure 1C. The production of RvD2 in bone marrow preceded its appearance in ischemic skeletal muscle; by day 5, levels of RvD2 were significantly increased in mice undergoing HLI in comparison with day 3 (Figure 1D). The increase in the production of RvD2 in skeletal muscle at day 5 was inversely related to its biosynthetic intermediate, 17-HDHA. Importantly, we also identified RvD2 in skeletal muscle biopsies from PAD patients, whereas RvD2 was absent in skeletal muscle of healthy individuals (Figure 1E and 1F).

Monocytes play an essential role in revascularization during HLI; hence, we asked whether they are a cellular source of RvD2. We found that CCR2$^+$ monocytes are recruited to skeletal muscle during HLI (day 3; Figure 1G). Splenic monocytes converted DHA to 17-HDHA and RvD2 (Figure 1H). This conversion was essentially abolished in monocytes isolated from *Alox15*$^{-/-}$ mice (Figure 1H), validating their enzymatic biosynthesis. Collectively, these results show that RvD2 is generated in a temporal manner during HLI and that monocytes are a potential cellular source of RvD2 during HLI.[29]

Tissue Perfusion and Arteriogenesis Are Enhanced by RvD2 During HLI

Given that RvD2 was generated in a temporal manner during HLI, we next asked whether therapeutic administration of RvD2 could enhance perfusion recovery. Previous studies have shown that exogenous RvD2 is effective at resolving inflammation in vivo at picogram-nanogram doses.[16,30] We began treatment at day 1, preceding its endogenous biosynthesis in skeletal muscle (Figure 1). With the use of laser Doppler perfusion imaging, mice undergoing HLI and treated with vehicle showed a time-dependent increase in tissue perfusion that reached ≈30% restoration of blood flow by day 14 post-HLI (Figure 2A and 2B). In contrast, mice treated with RvD2 showed significant improvement in perfusion that manifested by day 7 (Figure 2B). We visualized the limb vasculature by using Microfil casting and micro-CT. For this, we first used a milder model of HLI to limit endogenous arteriogenesis (see scheme in Figure 2C). Whole-mount imaging of vascular-casted limbs indicated that, in comparison with vehicle treatment, RvD2 increased the appearance of enlarged collateral vessels (Figure 2C). Quantification of vascular volume by micro-CT analysis revealed a significant increase by RvD2 (Figure 2D). In a more severe model of HLI that stimulates robust endogenous arteriogenesis (see scheme in Figure 2E), we found that RvD2 significantly enhanced vascular volume (Figure 2F) and the appearance of corkscrew-like collateral vessels (Figure 2E; indicated by white arrows). Collectively, these results show that RvD2 enhances perfusion during HLI, likely by increasing arteriogenesis.

RvD2 Resolves Inflammation and Promotes Tissue Regeneration During Revascularization

During acute inflammation, RvD2 hastens resolution by reducing neutrophil recruitment and proinflammatory cytokine production, and by enhancing macrophage efferocytosis (clearance of apoptotic cells), as well.[16,30] Because most prorevascularization mediators also enhance inflammation, we next sought to determine how exogenous RvD2 modulates the sterile inflammatory response during HLI. In comparison with sham controls, levels of neutrophils (Ly6G$^+$F4/80$^-$) increased significantly in skeletal muscle of mice undergoing HLI (Figure 3A through 3C). This increase was prevented in mice treated with RvD2, consistent with its defined role in regulating neutrophil trafficking (Figure 3A through 3C). In contrast, RvD2 did not affect tissue accumulation of monocytes or F4/80$^+$ macrophages, which play important roles in revascularization and tissue repair (Figure 3D and 3E and data not shown).[21,31] Consistent with the flow cytometry results, mRNA expression of *Emr1* (which encodes F4/80) was not affected by RvD2 in skeletal muscle of mice subjected to HLI (Figure 3F). Interestingly, RvD2 significantly decreased ischemia-induced increases in granulocyte macrophage colony-stimulating factor, and proinflammatory cytokine, tumor necrosis factor-α (Figure 3G). These early changes in inflammation and revascularization translated into markedly enhanced tissue regeneration in ischemic skeletal muscle, as evidenced by a significant increase in myocytes with centrally located nuclei at 14 days post-HLI (Figure 3H and 3I). These results indicate that RvD2 promotes the resolution of inflammation and tissue regeneration during HLI.

RvD2 Stimulates Endothelial Cell Migration in a Receptor and Rac-Dependent Manner

We previously reported that RvD2 regulates leukocyte-endothelial interactions in part via direct actions on endothelial cells, which are important contributors to arteriogenesis.[16,32] Here, we found that RvD2 enhanced endothelial cell migration in a concentration-dependent manner and to an extent similar to VEGF (Figure 4A and 4B). In contrast, RvD2 did not enhance endothelial cell proliferation, which was robustly stimulated by VEGF (Figure 4C). This lack of effect on proliferation was not due to a decrease in cell viability (Figure 4D). Matrigel plugs loaded with basic fibroblast growth factor showed a gross appearance consistent with angiogenesis, whereas control and RvD2-loaded plugs were essentially devoid of these structures (Figure 4E). Flow cytometry analysis of digested Matrigel demonstrated that basic fibroblast growth factor significantly increased the accumulation of CD31$^+$CD105$^+$ (endoglin$^+$) cells,[33] whereas their levels in RvD2-loaded plugs were not elevated

Circulation. 2016;134:666–680. DOI: 10.1161/CIRCULATIONAHA.116.021894

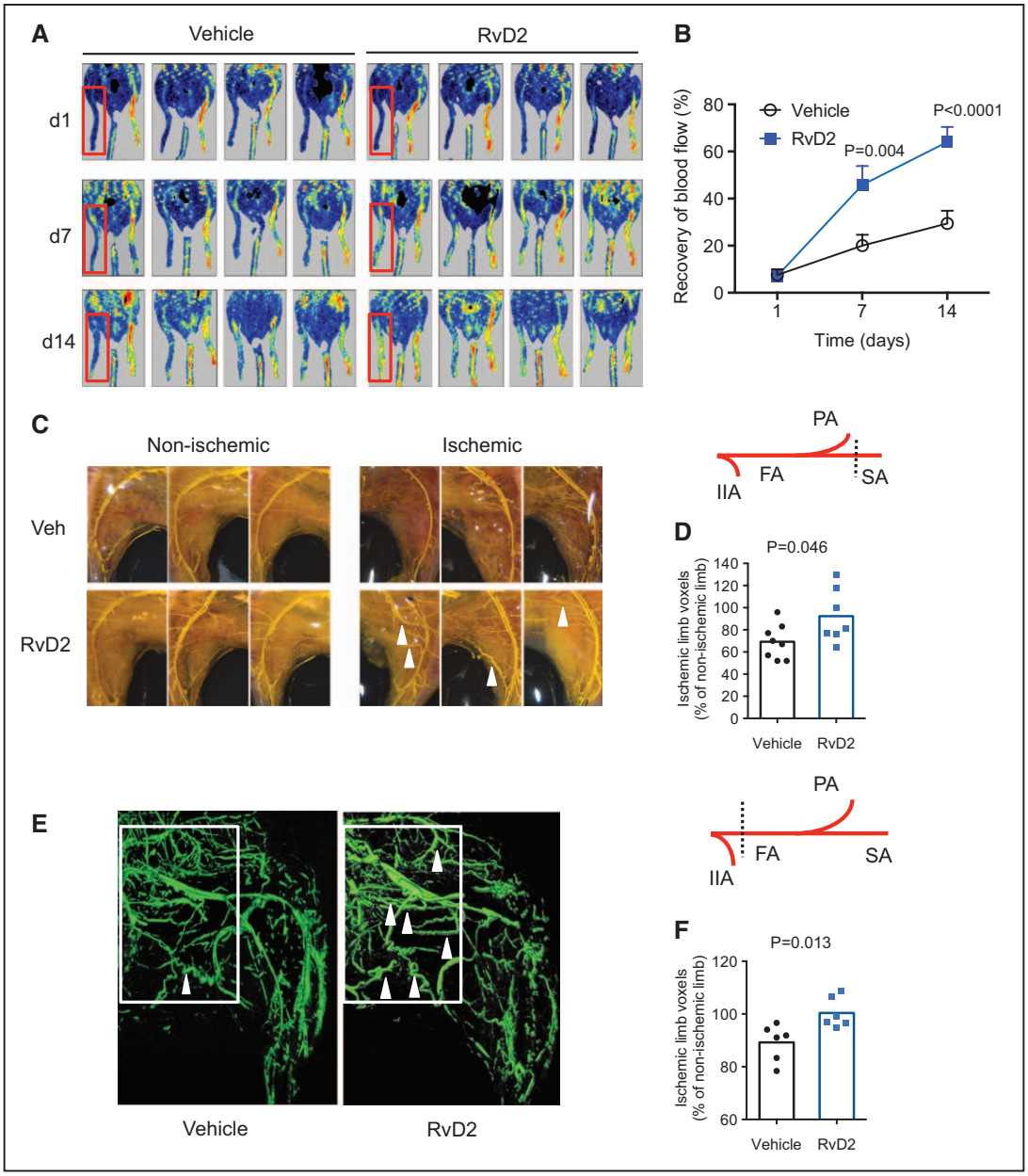

Figure 2. RvD2 enhances arteriogenesis during HLI.
A and **B,** Laser Doppler perfusion imaging of mice undergoing HLI and treated with vehicle or RvD2 for 14 days (d). Quantification of tissue perfusion in the ischemic limb (red box), presented as percentage of perfusion of the nonischemic limb is shown in **B**. **C,** Representative whole-mount images of Microfil vascular casted limbs of mice undergoing HLI and treated with vehicle or RvD2 for 3 days. A schematic of the ligation site is shown on the right. **D,** Quantification of vascular volume by micro-CT analysis. **E,** Representative micro-CT images showing the limb vasculature in mice undergoing HLI and treated with vehicle or RvD2 for 7 days. The white box indicates the region of interest with identification of corkscrew-like collateral vessels indicted by arrowheads. This more severe (proximal) ligation site is indicated in the schematic on the right. **F,** Quantification of vascular volume by micro-CT analysis. Data are mean±SEM; n=6 to 8/group. Statistical comparisons were made using a 2-way ANOVA, followed by Sidak multiple comparisons post hoc tests (**B**) or an unpaired 2-tailed Student *t* test (**D** and **F**). ANOVA indicates analysis of variance; FA, femoral artery; HLI, hind limb ischemia; IIA, internal iliac artery; micro-CT, microcomputed tomography; PA, popliteal artery; RvD2, resolvin D2; SA, saphenous artery; SEM, standard error of the mean; and Veh, vehicle.

above the control group, indicating that RvD2 does not stimulate angiogenesis (Figure 4F and 4G).

Some vasoactive mediators that regulate endothelial migration can also promote vascular permeability (eg, VEGF); thus, we assessed whether this process was affected by RvD2. As shown in Figure 4H, subcutaneous administration of RvD2 at the same dose used for HLI studies (see above) did not promote

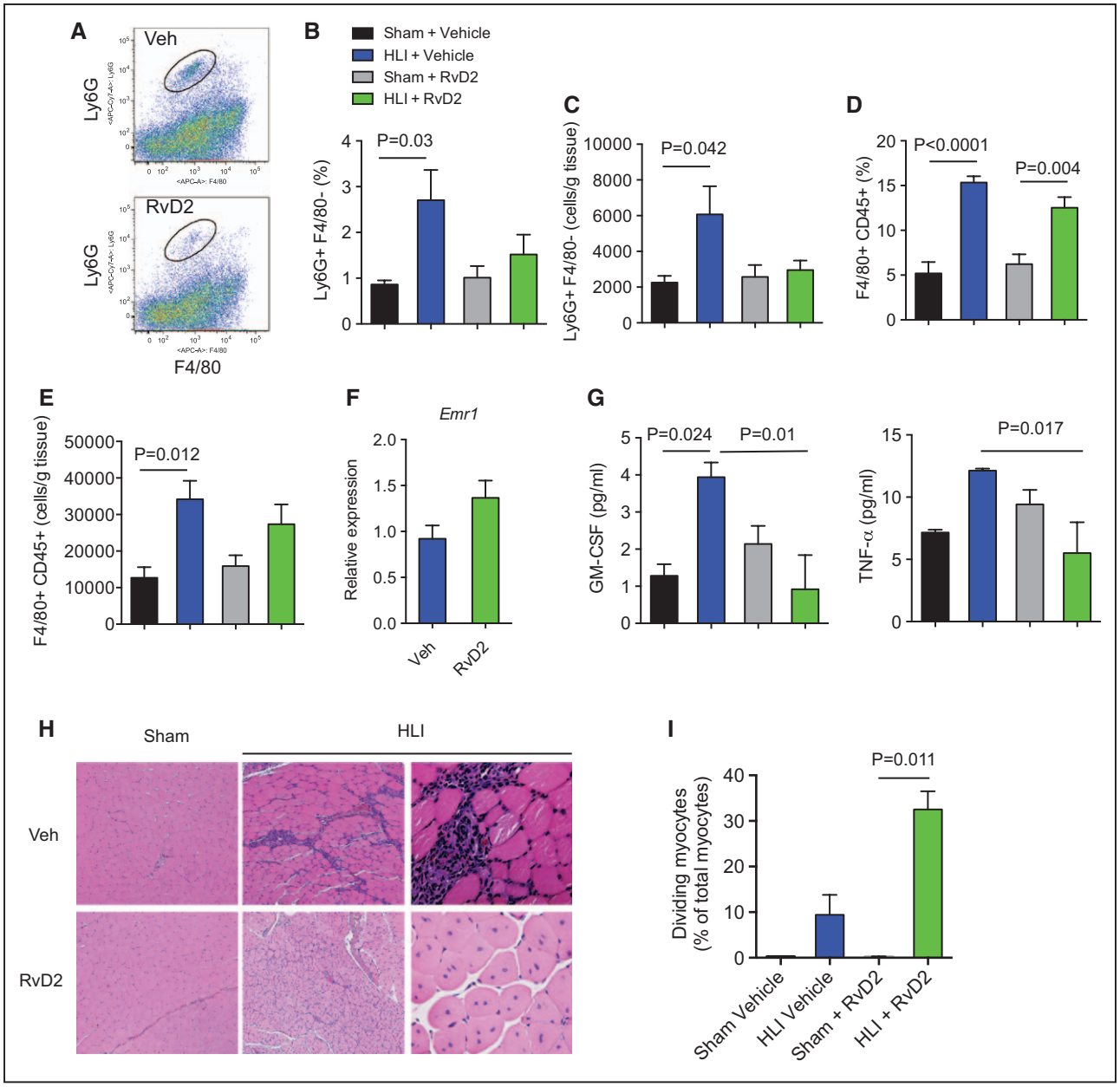

Figure 3. Therapeutic administration of RvD2 decreases inflammation and promotes tissue regeneration during HLI. **A,** Representative flow cytometry dot plots of Ly6G$^+$F4/80$^-$ neutrophils in mice undergoing HLI and treated with vehicle or RvD2. Quantification by flow cytometry of Ly6G$^+$ neutrophils (**B** and **C**) and F4/80$^+$CD45$^+$ macrophages (**D** and **E**) in skeletal muscle isolated from mice undergoing sham surgery or HLI (day 3) and treated with vehicle or RvD2. Results are presented as a percentage of total cells and total cells/g of tissue. **F,** Expression of *Emr1* (F4/80) in skeletal muscle of mice undergoing HLI and treated with vehicle or RvD2. **G,** Plasma levels of GM-CSF and TNFα in mice undergoing sham surgery or HLI and treated with vehicle or RvD2. **H,** Representative images (hematoxylin and eosin; 10× images in left and middle; 40× images in right) of skeletal muscle from mice undergoing sham surgery or HLI (day 14) and treated with vehicle or RvD2. **I,** Quantification of myocytes with centrally located nuclei in skeletal muscle. Data are mean±SEM; n=4 to 5/group. Multiple group comparisons were made using 1-way ANOVA, followed by Tukey multiple comparisons post hoc tests (**B** through **G**) or nonparametric 1-way ANOVA (Kruskal-Wallis), followed by Dunn multiple comparisons post hoc tests (**I**). ANOVA indicates analysis of variance; GM-CSF, granulocyte macrophage colony-stimulating factor; HLI, hind limb ischemia; RvD2, resolvin D2; SEM, standard error of the mean; TNF-α, tumor necrosis factor α; and Veh, vehicle.

leakage of Evan blue dye, whereas histamine markedly increased dye extravasation. These results, which are consistent with our previous studies using intravital microscopy,[16] suggest that RvD2 modulates endothelial cell function without increasing vascular permeability.

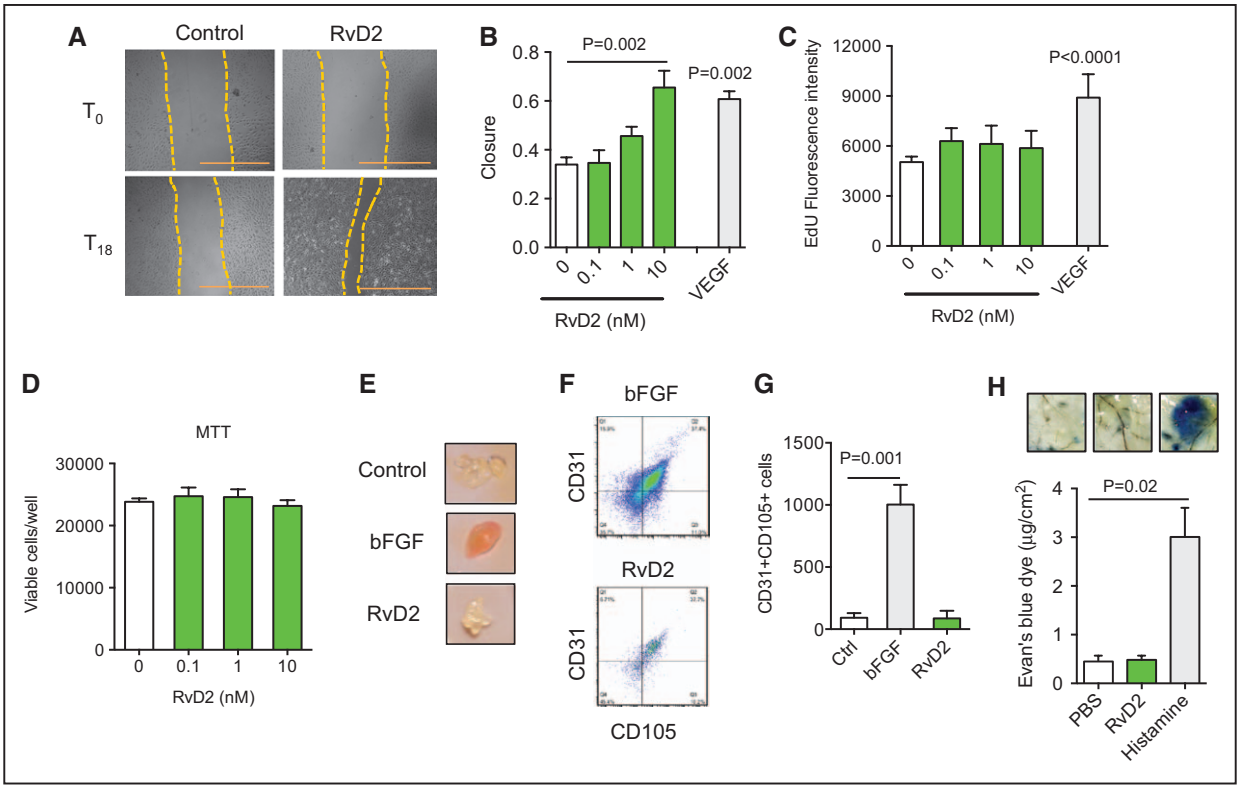

Figure 4. RvD2 stimulates endothelial cell migration but not proliferation.

A and **B,** Representative images (scale bar=1 mm) and quantification of endothelial cell migration in response to vehicle, RvD2, or VEGF-A (100 ng/mL). **C,** Proliferation assay (5-ethynyl-2′-deoxyuridine; EdU incorporation) of endothelial cells stimulated with RvD2 at indicated concentrations. **D,** Endothelial cell viability (MTT assay) in the presence of RvD2. **E,** Representative images of Matrigel plugs loaded with RvD2 or bFGF and excised from mice 7 days after implantation. **F,** Flow cytometry dot plots of $CD31^+CD105^+$ (endoglin$^+$) cells isolated from Matrigel plugs as in **F**. **G,** Quantification of $CD31^+CD105^+$ cells excised from Matrigel plugs. **H,** Assessment of vascular permeability (Evan blue dye extravasation) in mice given PBS, RvD2 or histamine, with representative images of subcutaneous tissue biopsies shown. Data are mean±SEM; n=3 to 6/group (**A** through **G**); n=4 to 6/group (**H**). Statistical comparisons were made using 1-way ANOVA, followed by Dunnett multiple comparisons post hoc tests (in comparison with control; **B**, **C**, **D**, and **G**), nonparametric 1-way ANOVA, followed by Dunn multiple comparisons post hoc tests (**H**), or an unpaired 2-tailed Student *t* test (VEGF versus Control; **B** and **C**). ANOVA indicates analysis of variance; bFGF, basic fibroblast growth factor; PBS, phosphate-buffered saline; RvD2, resolvin D2; SEM, standard error of the mean; VEFG, vascular endothelial growth factor; and Veh, vehicle.

Because RvD2 stimulated endothelial cell migration, we evaluated expression of its recently characterized specific receptor, GPR18.[30] Indeed, GPR18 (both protein and mRNA) was expressed in endothelial cells (Figure 5A and 5B) and *Gpr18* mRNA increased significantly on treatment with VEGF for 24 hours (Figure 5B). Stimulation of migration by RvD2 was completely abolished in cells pretreated with pertussis toxin (Figure 5C) and by specific GPR18 antagonist, O-1918[34] (Figure 5D). To identify mediators of RvD2 action, we examined Rho-GTPases, which play an important role in endothelial cell migration[35] and are stimulated in macrophages by LXA_4, another proresolving lipid mediator.[36] RvD2 significantly increased the amount of active, GTP-bound Rac (Figure 5E), and the promigratory effects of RvD2 were blocked with Rac inhibitor, NSC23766[37] (Figure 5F). Consistent with our previous results showing that RvD2 stimulates the production of nitric oxide in human endothelial cells and that these effects are pertussis toxin sensitive,[16] NOS inhibitor, N$^{\omega}$-nitro-L-arginine methyl ester, also blocked RvD2's promigratory actions (Figure 5F). Given the interplay between Rac and endothelial nitric oxide synthase in regulating endothelial cell migration,[38] these results suggest that RvD2 could affect migration by targeting the Rac/endothelial nitric oxide synthase pathway.

Deficiency of RvD2 Receptor, *Gpr18*, Impairs Perfusion During HLI

Our results demonstrate that, in addition to neutrophils and macrophages,[30] GPR18 is expressed in endothelial cells; we next evaluated whether genetic deficiency of *Gpr18* affects perfusion recovery during HLI. As shown

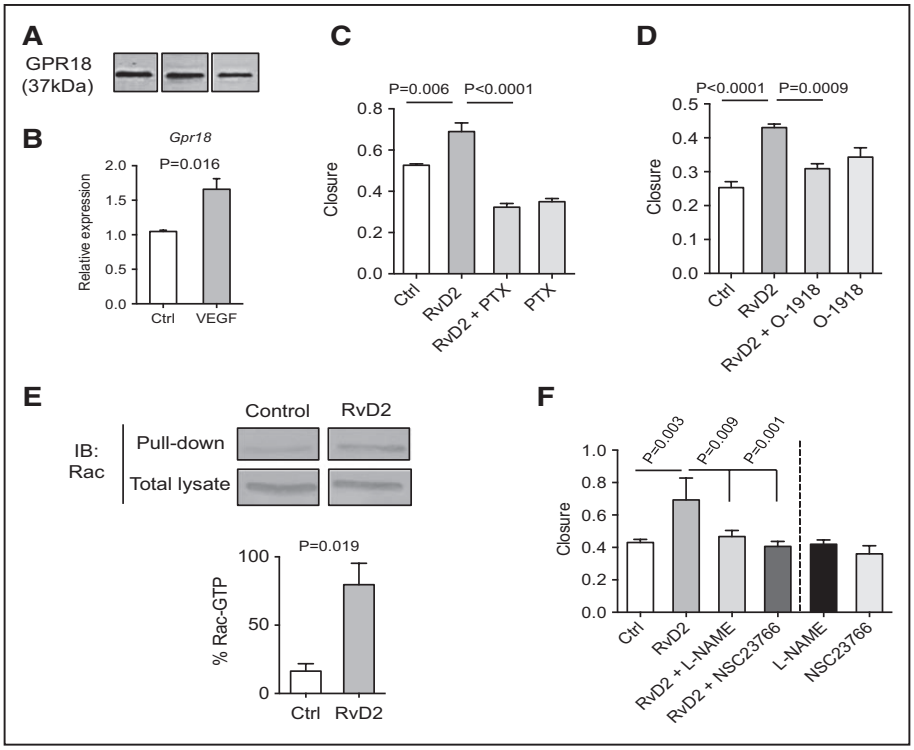

Figure 5. RvD2 promotes endothelial cell migration in a GPR18 and Rac-dependent manner.
A, Western blot of GPR18 (37 kDa) in endothelial cells. **B,** Levels of *Gpr18* transcripts in endothelial cells stimulated with VEGF-A (100 ng/mL) for 24 hours. **C** and **D,** Migration of endothelial cells stimulated with RvD2 (10 nmol/L) in cells pretreated with pertussis toxin (PTX; 1 μg/mL) or GPR18 inhibitor (O-1918; 20 μmol/L). **E,** Rac activation assay in endothelial cells stimulated with RvD2 (1 nmol/L; 30 minutes), with quantification of GTP-bound Rac shown in on the lower graph. **F,** Quantification of endothelial cell migration in cells pretreated with Rac inhibitor, NSC23766 (100 μmol/L) or nitric oxide synthase inhibitor, L-NAME (100 μmol/L), and then stimulated with RvD2 (10 nmol/L). Data are mean±SEM; n=3 to 6/group. Statistical comparisons were made using 1-way ANOVA, followed by Tukey multiple comparisons post hoc tests (**C**, **D**, and **F**) or an unpaired 2-tailed Student *t* test (**B** and **E**). ANOVA indicates analysis of variance; IB, immunoblot; L-NAME, N^{ω}-nitro-L-arginine methyl ester; RvD2, resolvin D2; SEM, standard error of the mean; and VEFG, vascular endothelial growth factor.

in Figure 6A, *Gpr18*-deficient mice had a marked endogenous defect in perfusion recovery during HLI in comparison with their WT littermates. Quantification of perfusion recovery showed that *Gpr18*-deficient mice recovered at a slower rate than their WT littermates and had significant defects in perfusion that manifested by day 7 post-HLI (Figure 6B and 6C). The defect in perfusion in *Gpr18*-deficient mice was not attributable to differences in limb perfusion at baseline.

RvD2 Rescues Defective Revascularization in Obese-Diabetic Mice

Chronic inflammation and metabolic disease impair the normal process of tissue revascularization, and diabetic patients are particularly susceptible to impaired tissue perfusion and wound healing.[1,2] Moreover, diabetic patients with PAD have higher rates of vein graft failure.[39] In animal models of diabetes mellitus, revascularization and arteriogenesis during HLI are impaired.[40,41] Thus, to test the translational relevance of our findings, we questioned whether RvD2 treatment could restore defective revascularization in diabetic mice. In comparison with WT mice, obese-diabetic mice (*db/db*) had a significant and sustained defect in revascularization during HLI (Figure 7). Treatment with RvD2 significantly increased tissue perfusion in *db/db* mice in comparison with vehicle-treated mice and to a level that was indistinguishable from WT mice by day 14 (Figure 7). These results demonstrate that, in addition to enhancing the rate of normal revascularization, RvD2 overcomes defective perfusion recovery in diabetes mellitus.

DISCUSSION

In this study, we found that RvD2 is generated in limb ischemia in both rodents and humans and that therapeutic administration of RvD2 enhances revascularization, while at the same time resolving inflammation. We identified the newly characterized receptor for RvD2 (ie, GPR18) in endothelial cells and found that RvD2 stimulates endothelial cell migration in a Rac-dependent manner. Taken together, these findings assign a new biological role to RvD2 in the revascularization program

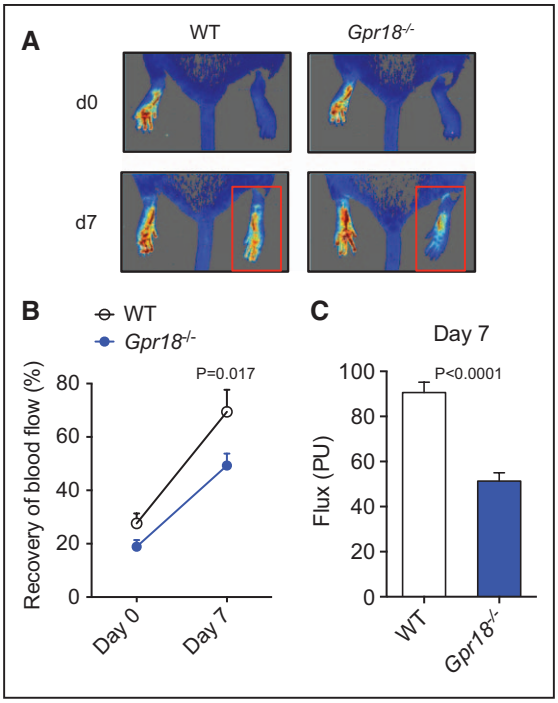

Figure 6. Deficiency of RvD2 receptor, *Gpr18*, impairs perfusion recovery during HLI.
A, Representative laser speckle perfusion imaging in WT and *Gpr18*-KO mice undergoing HLI (d0, day 0; d7, day 7). The red box indicates the ischemic limb. **B,** Quantification of limb perfusion in WT and *Gpr18*-KO mice undergoing HLI (percentage of perfusion relative to the nonischemic limb). **C,** Absolute flux (perfusion units [PU]) in the ischemic limbs of WT and *Gpr18*-KO mice at day 7. Data are mean±SEM; n=5 to 7/group. Statistical comparisons were made using 2-way ANOVA, followed by Sidak multiple comparisons post hoc tests (**B**) or an unpaired 2-tailed Student *t* test (**C**). ANOVA indicates analysis of variance; HLI, hind limb ischemia; RvD2, resolvin D2; SEM, standard error of the mean; and WT, wild type.

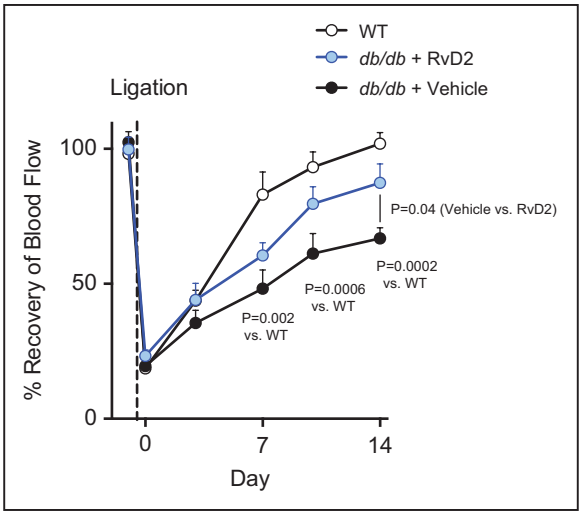

Figure 7. RvD2 rescues defective revascularization in diabetic mice.
Quantification of limb perfusion in WT or leptin receptor-deficient (*db/db*) mice undergoing HLI and treated with vehicle or RvD2 for 14 days. Results are presented as percentage of perfusion of the ischemic limb relative to the nonischemic limb. Data are mean±SEM; n=3 to 5/group. Statistical comparisons were made by using 2-way ANOVA, followed by Sidak multiple comparisons post hoc tests, with *P* values for specific comparisons indicated. ANOVA indicates analysis of variance; HLI, hind limb ischemia; RvD2, resolvin D2; SEM, standard error of the mean; and WT, wild type.

and could open up new directions for the development of novel therapeutic interventions for patients with PAD and CLI.

During infection, tissue injury, or ischemia, the inflammatory response is tightly coupled to the wound-healing program; immune cells combat pathogens and clear cellular debris to enable subsequent stages of tissue repair and regeneration. In this process, monocytes and macrophages are particularly important because they produce growth factors and other mediators that regulate cell migration, proliferation, and extracellular matrix remodeling.[42] Monocytes are mobilized from the bone marrow and the spleen during ischemia, preceding their accumulation in ischemic tissues.[28] We observed that RvD2 is produced in the bone marrow during ischemia and by isolated splenic monocytes in a lipoxygenase-dependent manner. Monocytes are necessary for revascularization during HLI,[8] and we found that RvD2 is sufficient to increase revascularization. These results are consistent with a previous study demonstrating that genetic deficiency of *Alox15* impairs perfusion during HLI,[43] although it should be noted that 12/15-LOX contributes to the biosynthesis of several other lipid mediators. Thus, in our study, we focused on direct actions of RvD2 and its receptor, GPR18, to understand the specific role of RvD2 in revascularization.

It is significant to point out that our results show that mediators that diminish inflammation can enhance revascularization. This is important because most previously identified interventions that promote revascularization also increase inflammation and atherosclerosis.[11,12] For instance, administration of monocyte chemoattractant protein 1 promotes monocyte recruitment and arteriogenesis during HLI, but also increases monocyte infiltration into atherosclerotic lesions and enhances lesion formation.[11] In contrast, interleukin-10 is an anti-inflammatory cytokine that is protective in atherosclerosis, but impairs revascularization during ischemia.[12,44] Our results challenge this paradigm by demonstrating that RvD2 both resolves inflammation and promotes revascularization. These findings lend further support to the notion that the effects of resolving inflammation are distinct from anti-inflammatory interventions, which are immunosuppressive. Because lipid mediators like resolvins are immunomodulatory, they decrease the production of proinflammatory me-

diators, while enhancing host defense (eg, macrophage phagocytosis of bacteria and apoptotic cells).[14] Indeed, we found that RvD2 did not promote vascular permeability or macrophage accumulation in skeletal muscle, but reduced neutrophil accumulation and tumor necrosis factor-α and granulocyte macrophage colony-stimulating factor production. These effects were associated with improved revascularization and enhanced skeletal muscle regeneration, suggesting that, unlike anti-inflammatory drugs, RvD2 has a dual effect, diminishing inflammation and promoting wound healing. We note that, similar to other recent studies,[20,21] we ligated both the artery and vein to prevent damaging the associated nerve and to preserve limb function. Ligating the vein in addition to the artery may change the duration or mechanisms of perfusion recovery. However, the extent of perfusion recovery determined in our study is similar to that observed by other groups in which only the artery is ligated.[8,40] In future studies, it may be important to determine how RvD2 affects perfusion in contexts that more closely mirror impaired perfusion in humans (eg, atherosclerosis), and to determine how long-term treatment with RvD2 regulates later phases of tissue remodeling.

Promotion of the resolution of inflammation by RvD2 overcomes a critical barrier to revascularization therapy, ie, chronic inflammation, which in PAD impairs endogenous revascularization and limits the effectiveness of prorevascularization therapies.[7] Indeed, several inflammatory mediators, including tumor necrosis factor-α, are associated with poor clinical outcomes in PAD.[45] Moreover, accumulating evidence indicates that resolvins may also reduce atherosclerosis and pathological restenosis.[17,46,47] The notion that resolving inflammation is critical for promoting revascularization is supported by our previous observation that plasma levels of another proresolving mediator, 15-epi-LXA$_4$, are inversely correlated with PAD severity (ie, intermittent claudication versus CLI) in humans.[13,48] Moreover, several chronic inflammatory diseases, including diabetes mellitus, obesity, and asthma are associated with impaired production of proresolving mediators.[13,49] Our results demonstrating that RvD2 rescues defective revascularization in diabetic mice are thus a significant step toward clinical translation. In future studies it will be important to determine whether impaired revascularization in conditions such as diabetes mellitus and PAD is causally related to an imbalance in proinflammatory versus proresolving mediators and whether treatment with resolvins could be a clinically useful approach to promoting revascularization.

In addition to resolving inflammation, we found that RvD2 directly stimulates endothelial cell migration by activating Rac. We identified the RvD2 receptor, GPR18, on endothelial cells and found that GPR18 mediates the promigratory actions of RvD2. Interestingly, *Gpr18*-deficient mice had endogenous defects in revascularization. Thus, in addition to regulating leukocyte trafficking during acute inflammation,[30] GPR18 may play a role in endothelial cell function. In further support of this concept, previous studies have determined that *Gpr18* is expressed in human endothelial cells and regulates activation of protein kinase B/AKT in a pertussis toxin–sensitive manner.[50] Moreover, RvD2 was recently found to stimulate AKT phosphorylation in human endothelial cells.[51] We note that, unlike growth factors, RvD2 did not stimulate endothelial cell proliferation, vascular permeability, or angiogenesis. In fact, previous studies have shown that pathological neovascularization is inhibited by resolvins.[52] This property of proresolving mediators could be particularly beneficial in the context of atherosclerosis and cancer, where angiogenesis could fuel disease progression.

In summary, the results of this study uncover a new role of resolvins in tissue revascularization following ischemic injury and suggest that resolution of inflammation is an important component of the revascularization program. Because impaired tissue vascularization is associated with chronic inflammation in diseases such as PAD and diabetes mellitus, these results could have important implications for revascularization therapy.

ACKNOWLEDGMENTS

The authors thank Charles N. Serhan and Nan Chiang (Harvard Medical School and Brigham and Women's Hospital) for assistance with experiments involving the *Gpr18*-deficient mice.

SOURCES OF FUNDING

This work was supported in part by NIH grants HL106173, GM095467 (to Dr Spite) and GM103492 (to Drs Bhatnagar, Spite, and Conklin). Dr Hellmann is the recipient of a National Research Service Award from the National Heart, Lung and Blood Institute, NIH (HL116186).

DISCLOSURES

None.

AFFILIATIONS

From Center for Experimental Therapeutics and Reperfusion Injury, Department of Anesthesiology, Perioperative and Pain Medicine, Brigham and Women's Hospital and Harvard Medical School, Harvard Institutes of Medicine, Boston, MA (B.E.S., J.H., M.S.); Institute of Molecular Cardiology, Diabetes and Obesity Center, Division of Cardiovascular Medicine, University of Louisville School of Medicine, Louisville, KY (M.J.Z., J.F.B., L.G., D.J.C., A.B.); and Vascular Medicine Section, Cardiovascular Division, Brigham and Women's Hospital and Harvard

Medical School, Boston, MA (C.M.P., J.C.P., M.A.C.). The current address for Dr Creager is Dartmouth-Hitchcock Heart and Vascular Center, Dartmouth College, Hanover, NH.

FOOTNOTES

Received November 6, 2015; accepted June 24, 2016.
Guest Editor for this article was Donald D. Heistad, MD.
Circulation is available at http://circ.ahajournals.org.

REFERENCES

1. Vartanian SM, Conte MS. Surgical intervention for peripheral arterial disease. *Circ Res*. 2015;116:1614–1628. doi: 10.1161/CIRCRESAHA.116.303504.
2. Bonaca MP, Creager MA. Pharmacological treatment and current management of peripheral artery disease. *Circ Res*. 2015;116:1579–1598. doi: 10.1161/CIRCRESAHA.114.303505.
3. Criqui MH, Aboyans V. Epidemiology of peripheral artery disease. *Circ Res*. 2015;116:1509–1526. doi: 10.1161/CIRCRESAHA.116.303849.
4. Chilian WM, Penn MS, Pung YF, Dong F, Mayorga M, Ohanyan V, Logan S, Yin L. Coronary collateral growth–back to the future. *J Mol Cell Cardiol*. 2012;52:905–911. doi: 10.1016/j.yjmcc.2011.12.006.
5. Faber JE, Chilian WM, Deindl E, van Royen N, Simons M. A brief etymology of the collateral circulation. *Arterioscler Thromb Vasc Biol*. 2014;34:1854–1859. doi: 10.1161/ATVBAHA.114.303929.
6. Simons M, Eichmann A. Molecular controls of arterial morphogenesis. *Circ Res*. 2015;116:1712–1724. doi: 10.1161/CIRCRESAHA.116.302953.
7. Cooke JP, Losordo DW. Modulating the vascular response to limb ischemia: angiogenic and cell therapies. *Circ Res*. 2015;116:1561–1578. doi: 10.1161/CIRCRESAHA.115.303565.
8. Heil M, Ziegelhoeffer T, Wagner S, Fernández B, Helisch A, Martin S, Tribulova S, Kuziel WA, Bachmann G, Schaper W. Collateral artery growth (arteriogenesis) after experimental arterial occlusion is impaired in mice lacking CC-chemokine receptor-2. *Circ Res*. 2004;94:671–677. doi: 10.1161/01.RES.0000122041.73808.B5.
9. Jetten N, Donners MM, Wagenaar A, Cleutjens JP, van Rooijen N, de Winther MP, Post MJ. Local delivery of polarized macrophages improves reperfusion recovery in a mouse hind limb ischemia model. *PLoS One*. 2013;8:e68811. doi: 10.1371/journal.pone.0068811.
10. Kuwahara G, Nishinakamura H, Kojima D, Tashiro T, Kodama S. GM-CSF treated F4/80+ BMCs improve murine hind limb ischemia similar to M-CSF differentiated macrophages. *PLoS One*. 2014;9:e106987. doi: 10.1371/journal.pone.0106987.
11. van Royen N, Hoefer I, Böttinger M, Hua J, Grundmann S, Voskuil M, Bode C, Schaper W, Buschmann I, Piek JJ. Local monocyte chemoattractant protein-1 therapy increases collateral artery formation in apolipoprotein E-deficient mice but induces systemic monocytic CD11b expression, neointimal formation, and plaque progression. *Circ Res*. 2003;92:218–225.
12. Epstein SE, Stabile E, Kinnaird T, Lee CW, Clavijo L, Burnett MS. Janus phenomenon: the interrelated tradeoffs inherent in therapies designed to enhance collateral formation and those designed to inhibit atherogenesis. *Circulation*. 2004;109:2826–2831. doi: 10.1161/01.CIR.0000132468.82942.F5.
13. Serhan CN, Chiang N, Dalli J. The resolution code of acute inflammation: Novel pro-resolving lipid mediators in resolution. *Semin Immunol*. 2015;27:200–215. doi: 10.1016/j.smim.2015.03.004.
14. Serhan CN. Pro-resolving lipid mediators are leads for resolution physiology. *Nature*. 2014;510:92–101. doi: 10.1038/nature13479.
15. Spite M, Serhan CN. Novel lipid mediators promote resolution of acute inflammation: impact of aspirin and statins. *Circ Res*. 2010;107:1170–1184. doi: 10.1161/CIRCRESAHA.110.223883.
16. Spite M, Norling LV, Summers L, Yang R, Cooper D, Petasis NA, Flower RJ, Perretti M, Serhan CN. Resolvin D2 is a potent regulator of leukocytes and controls microbial sepsis. *Nature*. 2009;461:1287–1291. doi: 10.1038/nature08541.
17. Merched AJ, Ko K, Gotlinger KH, Serhan CN, Chan L. Atherosclerosis: evidence for impairment of resolution of vascular inflammation governed by specific lipid mediators. *FASEB J*. 2008;22:3595–3606. doi: 10.1096/fj.08-112201.
18. Norling LV, Dalli J, Flower RJ, Serhan CN, Perretti M. Resolvin D1 limits polymorphonuclear leukocyte recruitment to inflammatory loci: receptor-dependent actions. *Arterioscler Thromb Vasc Biol*. 2012;32:1970–1978. doi: 10.1161/ATVBAHA.112.249508.
19. Limbourg A, Korff T, Napp LC, Schaper W, Drexler H, Limbourg FP. Evaluation of postnatal arteriogenesis and angiogenesis in a mouse model of hind-limb ischemia. *Nat Protoc*. 2009;4:1737–1746. doi: 10.1038/nprot.2009.185.
20. Kim JA, March K, Chae HD, Johnstone B, Park SJ, Cook T, Merfeld-Clauss S, Broxmeyer HE. Muscle-derived Gr1(dim)CD11b(+) cells enhance neovascularization in an ischemic hind limb mouse model. *Blood*. 2010;116:1623–1626. doi: 10.1182/blood-2009-08-237040.
21. Takeda Y, Costa S, Delamarre E, Roncal C, Leite de Oliveira R, Squadrito ML, Finisguerra V, Deschoemaeker S, Bruyère F, Wenes M, Hamm A, Serneels J, Magat J, Bhattacharyya T, Anisimov A, Jordan BF, Alitalo K, Maxwell P, Gallez B, Zhuang ZW, Saito Y, Simons M, De Palma M, Mazzone M. Macrophage skewing by Phd2 haplodeficiency prevents ischaemia by inducing arteriogenesis. *Nature*. 2011;479:122–126. doi: 10.1038/nature10507.
22. Traktuev DO, Tsokolaeva ZI, Shevelev AA, Talitskiy KA, Stepanova VV, Johnstone BH, Rahmat-Zade TM, Kapustin AN, Tkachuk VA, March KL, Parfyonova YV. Urokinase gene transfer augments angiogenesis in ischemic skeletal and myocardial muscle. *Mol Ther*. 2007;15:1939–1946. doi: 10.1038/sj.mt.6300262.
23. Simons M, Alitalo K, Annex BH, Augustin HG, Beam C, Berk BC, Byzova T, Carmeliet P, Chilian W, Cooke JP, Davis GE, Eichmann A, Iruela-Arispe ML, Keshet E, Sinusas AJ, Ruhrberg C, Woo YJ, Dimmeler S; American Heart Association Council on Basic Cardiovascular Sciences and Council on Cardiovascular Surgery and Anesthesia. State-of-the-art methods for evaluation of angiogenesis and tissue vascularization: a scientific statement from the American Heart Association. *Circ Res*. 2015;116:e99–e132. doi: 10.1161/RES.0000000000000054.
24. Ciciliot S, Schiaffino S. Regeneration of mammalian skeletal muscle. Basic mechanisms and clinical implications. *Curr Pharm Des*. 2010;16:906–914.
25. Colas RA, Shinohara M, Dalli J, Chiang N, Serhan CN. Identification and signature profiles for pro-resolving and inflammatory lipid mediators in human tissue. *Am J Physiol Cell Physiol*. 2014;307:C39–C54. doi: 10.1152/ajpcell.00024.2014.
26. Miles AA, Miles EM. Vascular reactions to histamine, histamine-liberator and leukotaxine in the skin of guinea-pigs. *J Physiol*. 1952;118:228–257.
27. Mikelis CM, Simaan M, Ando K, Fukuhara S, Sakurai A, Amornphimoltham P, Masedunskas A, Weigert R, Chavakis T, Adams RH, Offermanns S, Mochizuki N, Zheng Y, Gutkind JS. RhoA and ROCK mediate histamine-induced vascular leakage and anaphylactic shock. *Nat Commun*. 2015;6:6725. doi: 10.1038/ncomms7725.
28. Swirski FK, Nahrendorf M. Leukocyte behavior in atherosclerosis, myocardial infarction, and heart failure. *Science*. 2013;339:161–166. doi: 10.1126/science.1230719.
29. Mirakaj V, Dalli J, Granja T, Rosenberger P, Serhan CN. Vagus nerve controls resolution and pro-resolving mediators of inflammation. *J Exp Med*. 2014;211:1037–1048. doi: 10.1084/jem.20132103.

30. Chiang N, Dalli J, Colas RA, Serhan CN. Identification of resolvin D2 receptor mediating resolution of infections and organ protection. *J Exp Med*. 2015;212:1203–1217. doi: 10.1084/jem.20150225.
31. Arnold L, Henry A, Poron F, Baba-Amer Y, van Rooijen N, Plonquet A, Gherardi RK, Chazaud B. Inflammatory monocytes recruited after skeletal muscle injury switch into antiinflammatory macrophages to support myogenesis. *J Exp Med*. 2007;204:1057–1069. doi: 10.1084/jem.20070075.
32. Moraes F, Paye J, Mac Gabhann F, Zhuang ZW, Zhang J, Lanahan AA, Simons M. Endothelial cell-dependent regulation of arteriogenesis. *Circ Res*. 2013;113:1076–1086. doi: 10.1161/CIRCRESAHA.113.301340.
33. Duff SE, Li C, Garland JM, Kumar S. CD105 is important for angiogenesis: evidence and potential applications. *FASEB J*. 2003;17:984–992. doi: 10.1096/fj.02-0634rev.
34. McHugh D, Hu SS, Rimmerman N, Juknat A, Vogel Z, Walker JM, Bradshaw HB. N-arachidonoyl glycine, an abundant endogenous lipid, potently drives directed cellular migration through GPR18, the putative abnormal cannabidiol receptor. *BMC Neurosci*. 2010;11:44. doi: 10.1186/1471-2202-11-44.
35. Tzima E. Role of small GTPases in endothelial cytoskeletal dynamics and the shear stress response. *Circ Res*. 2006;98:176–185. doi: 10.1161/01.RES.0000200162.94463.d7.
36. Maderna P, Cottell DC, Berlasconi G, Petasis NA, Brady HR, Godson C. Lipoxins induce actin reorganization in monocytes and macrophages but not in neutrophils: differential involvement of rho GTPases. *Am J Pathol*. 2002;160:2275–2283. doi: 10.1016/S0002-9440(10)61175-3.
37. Gao Y, Dickerson JB, Guo F, Zheng J and Zheng Y. Rational design and characterization of a Rac GTPase-specific small molecule inhibitor. *Proc Natl Acad Sci USA*. 2004;101:7618–23.
38. Sawada N, Salomone S, Kim HH, Kwiatkowski DJ, Liao JK. Regulation of endothelial nitric oxide synthase and postnatal angiogenesis by Rac1. *Circ Res*. 2008;103:360–368. doi: 10.1161/CIRCRESAHA.108.178897.
39. Owens CD, Ho KJ, Conte MS. Lower extremity vein graft failure: a translational approach. *Vasc Med*. 2008;13:63–74. doi: 10.1177/1358863X07083432.
40. Schiekofer S, Galasso G, Sato K, Kraus BJ, Walsh K. Impaired revascularization in a mouse model of type 2 diabetes is associated with dysregulation of a complex angiogenic-regulatory network. *Arterioscler Thromb Vasc Biol*. 2005;25:1603–1609. doi: 10.1161/01.ATV.0000171994.89106.ca.
41. van Golde JM, Ruiter MS, Schaper NC, Vöö S, Waltenberger J, Backes WH, Post MJ, Huijberts MS. Impaired collateral recruitment and outward remodeling in experimental diabetes. *Diabetes*. 2008;57:2818–2823. doi: 10.2337/db08-0229.
42. Mantovani A, Biswas SK, Galdiero MR, Sica A, Locati M. Macrophage plasticity and polarization in tissue repair and remodelling. *J Pathol*. 2013;229:176–185. doi: 10.1002/path.4133.
43. Singh NK, Kundumani-Sridharan V, Rao GN. 12/15-Lipoxygenase gene knockout severely impairs ischemia-induced angiogenesis due to lack of Rac1 farnesylation. *Blood*. 2011;118:5701–5712. doi: 10.1182/blood-2011-04-347468.
44. Silvestre JS, Mallat Z, Duriez M, Tamarat R, Bureau MF, Scherman D, Duverger N, Branellec D, Tedgui A, Levy BI. Antiangiogenic effect of interleukin-10 in ischemia-induced angiogenesis in mice hindlimb. *Circ Res*. 2000;87:448–452.
45. Pande RL, Brown J, Buck S, Redline W, Doyle J, Plutzky J, Creager MA. Association of monocyte tumor necrosis factor α expression and serum inflammatory biomarkers with walking impairment in peripheral artery disease. *J Vasc Surg*. 2015;61:155–161. doi: 10.1016/j.jvs.2014.06.116.
46. Akagi D, Chen M, Toy R, Chatterjee A, Conte MS. Systemic delivery of proresolving lipid mediators resolvin D2 and maresin 1 attenuates intimal hyperplasia in mice. *FASEB J*. 2015;29:2504–2513. doi: 10.1096/fj.14-265363.
47. Hasturk H, Abdallah R, Kantarci A, Nguyen D, Giordano N, Hamilton J, Van Dyke TE. Resolvin E1 (RvE1) Attenuates Atherosclerotic Plaque Formation in Diet and Inflammation-Induced Atherogenesis. *Arterioscler Thromb Vasc Biol*. 2015;35:1123–1133. doi: 10.1161/ATVBAHA.115.305324.
48. Ho KJ, Spite M, Owens CD, Lancero H, Kroemer AH, Pande R, Creager MA, Serhan CN, Conte MS. Aspirin-triggered lipoxin and resolvin E1 modulate vascular smooth muscle phenotype and correlate with peripheral atherosclerosis. *Am J Pathol*. 2010;177:2116–2123. doi: 10.2353/ajpath.2010.091082.
49. Spite M, Clària J, Serhan CN. Resolvins, specialized proresolving lipid mediators, and their potential roles in metabolic diseases. *Cell Metab*. 2014;19:21–36. doi: 10.1016/j.cmet.2013.10.006.
50. Offertáler L, Mo FM, Bátkai S, Liu J, Begg M, Razdan RK, Martin BR, Bukoski RD, Kunos G. Selective ligands and cellular effectors of a G protein-coupled endothelial cannabinoid receptor. *Mol Pharmacol*. 2003;63:699–705.
51. Maekawa T, Hosur K, Abe T, Kantarci A, Ziogas A, Wang B, Van Dyke TE, Chavakis T, Hajishengallis G. Antagonistic effects of IL-17 and D-resolvins on endothelial Del-1 expression through a GSK-3β-C/EBPβ pathway. *Nat Commun*. 2015;6:8272. doi: 10.1038/ncomms9272.
52. Connor KM, SanGiovanni JP, Lofqvist C, Aderman CM, Chen J, Higuchi A, Hong S, Pravda EA, Majchrzak S, Carper D, Hellstrom A, Kang JX, Chew EY, Salem N Jr, Serhan CN, Smith LE. Increased dietary intake of omega-3-polyunsaturated fatty acids reduces pathological retinal angiogenesis. *Nat Med*. 2007;13:868–873. doi: 10.1038/nm1591.